Journal of Modern Physics, 2013, 4, 622-627
http://dx.doi.org/10.4236/jmp.2013.45090 Published Online May 2013 (http://www.scirp.org/journal/jmp)

Long-Range Correlation in Positron-Hydrogen Scattering System near the Threshold of *Ps*(*n* = 2) Formation

Chi Yu Hu[1], David Caballero[1,2]
[1]Department of Physics and Astronomy, California State University, Long Beach, USA
[2]Claremont Graduate University, Claremont, USA
Email: chihu@csulb.edu

Received February 24, 2013; revised March 28, 2013; accepted April 20, 2013

ABSTRACT

This is a short report of a recently uncovered resonant phenomenon. The modified Faddeev equation that correctly includes all six open channels is used. The calculation is carried out in *s*-partial wave. We report a number of resonant peaks in the elastic cross sections as well as the wave amplitudes involved. This is the energy region where the Stark-effect induced electric dipole energy split in the target dominates the physics and the Long-Range behavior of the 3-body scattering system. It is found that when the center of mass collision energy in the new channels is in integer proportion to the corresponding electric dipole energy split, Bremsstrahlung photon mediated resonant scattering occurs. The corresponding wave amplitudes deform into wave-packets hundreds to thousands of Bohr radii in width. The physical implication of this phenomenon will be discussed.

Keywords: Faddeev; Resonance; Cross Section; 3-Body Scattering

1. Introduction

In a previous work [1], resonant formation of anti-hydrogen was reported for the charge-conjugate rearrangement scattering channels

$$\bar{P} + Ps(n=2) \to e^- + \bar{H}(n \le 2)$$

However, the physical origin of these resonances was not discussed with sufficient detail. In this work, we investigate the same resonances using the elastic scattering cross sections with the intent to identify the physical mechanism responsible for these resonances.

Gailitis and Damburg [2] discussed similar resonances in electron-Hydrogen scattering systems. They conjectured that this was a special case of Levinson theorem [3]. Since the induced dipole potential well produced a number of well known "bound-states", the Feshbach resonances [4-10] just belowed the threshold of $Ps(n=2)$ formation, then Levinson theorem predicts the same number of phase shift oscillations exist just above the same threshold. Present calculation indeed confirms that their conjecture was correct.

2. Brief Description of the Calculation

For the present *s*-wave calculation, there are six open channels in this energy region. The six elastic scattering channels are:

$$e^+ + H(n=1) \quad (1)$$

$$e^+ + H(n=2, \ell=0) \quad (2)$$

$$e^+ + H(n=2, \ell=1) \quad (3)$$

$$P + Ps(n=1) \quad (4)$$

$$P + Ps(n=2, \ell=0) \quad (5)$$

$$P + Ps(n=2, \ell=1) \quad (6)$$

The first (1)-(3) belong to Faddeev channel #1, the next (4)-(6) belong to Faddeev channel #2. In the figures, their cross sections are represented by σ_{ii} while i = 1, 6 in the order listed above.

Thirty four energy points are calculated in an energy range of $5.0\times10^{-4}\,Ry$. The modified Faddeev equations are solved using a combination of partial wave expansion and quintic spline collocation method [1,11,12]. In this representation the *s*-partial wave solutions are obtained by solving a linear equation system, with N = 387936 − 488808. N is the number of linear equations.

The cut-off distance for the first Faddeev channel is 500 α_0, for the second Faddeev channel is 1000 α_0. α_0 is

the Bohr radius. The two body bound states cut-off distances are determined separately such that the grids faithfully reproduce the Hydrogen or Positronium binding energy and wave function up to $n=2$.

3. Presentation of the Results

The six dimensional matrix $K_{ij}=\tan\delta_{ij}$, and all cross section matrix σ_{ij} are calculated. δ_{ij} is the phase shift matrix element for the incoming channel *i* and the outgoing channel *j*. The indexes *i*, *j* run from one to six according to the order listed in Equations (1)-(6).

K_{55} and K_{66} are shown in **Figure 1**. Both curves show that at a number of energy points the phase shift becomes zero from 0^+ to 0^-. While between a pair of adjacent crossing, the phase shift suddenly jumps from $-\pi/2$ to $\pi/2$. This shows that the incoming particle is subjected to sudden repulsion while approaching resonant configuration.

Figures 2 and **3** show that all the elastic cross sections

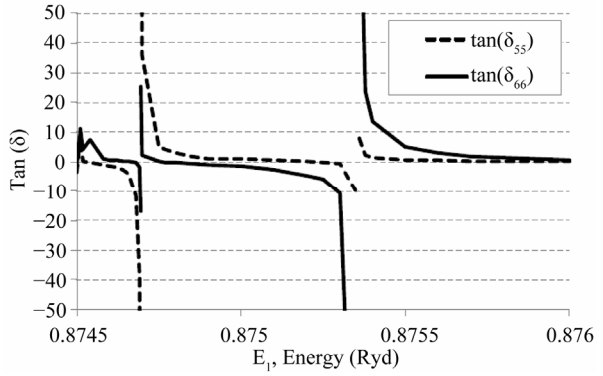

Figure 1. The diagonal matrix elements $K_{55}=\tan(\delta_{55})$ and $K_{66}=\tan(\delta_{66})$ are plotted against E_1, the energy of channel (1). Singularities occur between E_1 = 0.874694 − 0.874695*Ry* and $E_1=0.87535-0.87536Ry$ for both K_{55} and K_{66} respectively.

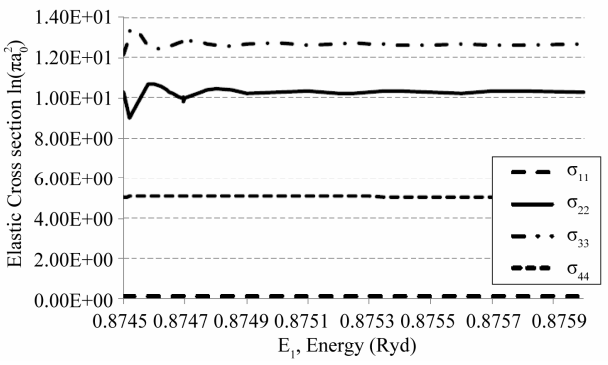

Figure 2. The elastic cross sections of channels 1-4 are plotted against E_1, the energy of channel (1). All four cross sections vary little in the energy range plotted.

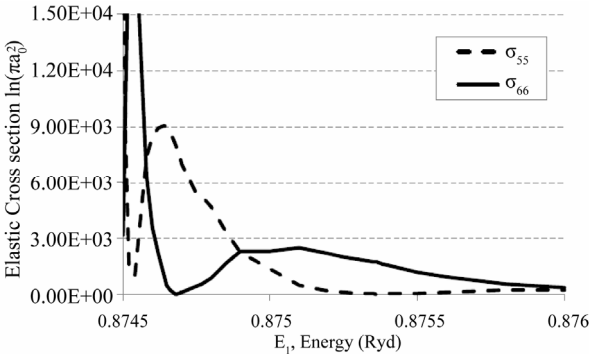

Figure 3. The elastic cross sections of channels 5 and channel 6 are plotted against E_1, the energy of channel (1). On the energy range plotted, channel 5 displays one large resonant peak. Located between $E_1\sim0.87464-0.87465Ry$. Two resonant peaks are found in channel (6) located at $E_1\sim0.87452-0.87454Ry$ and $E_1\sim0.875-0.8751Ry$ respectively.

are relatively smooth across the energy region except σ_{55} and σ_{66}. Apparently, there is a large cross section peak associated with each *K*-matrix singularity at slightly shifted energy locations. The *K*-matrix singularity associated with the much narrower third cross section peak at the lowest energy side is too narrow to be calculated at the present energy grid.

For easy comparison with previous references, the energy of channel (1), E_1, is used in **Figures 1-3**. E_1 is measured from the $H(1s)$ threshold. This energy differs slightly from the infinite proton mass values. The scattering wave function of the 3-body system is divided into two Faddeev amplitudes $\psi=\psi_1(\boldsymbol{x}_1,\boldsymbol{y}_1)+\psi_2(\boldsymbol{x}_2,\boldsymbol{y}_2)$. $\boldsymbol{x}_1,\boldsymbol{y}_1$ are the Jacobi vectors for the e^++H and $\boldsymbol{x}_2,\boldsymbol{y}_2$ are the Jacobi vectors for the $P+Ps$.

In the energy region considered, all elastic cross sections involving Faddeev amplitude $\psi_1(\boldsymbol{x}_1,\boldsymbol{y}_1)$, namely the channels (1), (2), and (3), are relatively smooth (see **Figure 2**). Resonances appear only in channels (5) and (6), (see **Figure 3**). They belong to Faddeev amplitude $\psi_2(\boldsymbol{x}_2,\boldsymbol{y}_2)$.

Channels (5) and (6) are the newly opened channels with energy very close to the threshold of $Ps(n=2)$ formation. Except in the immediate neighborhood of the *K*-matrix singularities, they are poorly coupled with the channels in $\psi_1(\boldsymbol{x}_1,\boldsymbol{y}_1)$ The energies of the latter channels lie orders of magnitudes higher above their respective thresholds than that of the new channels. As a result, the Faddeev amplitudes of channel (5) and (6) are three to four orders of magnitude larger than that belongs to $\psi_1(\boldsymbol{x}_1,\boldsymbol{y}_1)$. Numerically the total wave function $\psi\approx\psi_2(\boldsymbol{x}_2,\boldsymbol{y}_2)$, thus only $\psi_2(\boldsymbol{x}_2,\boldsymbol{y}_2)$ are used in the Figures below. However, **Figures 1** and **3** show that the

coupling of all six channels produces noticeable energy shifts between the peaks of the cross sections in **Figure 3** and the corresponding *K*-matrix singularities in **Figure 1**.

Figures 4 and **5** display plots of $\psi_2(x_2, y_2)$ for channels (5) and (6) respectively at an energy $E_1 = 0.875Ry$. This energy is near the peak of the first resonance to the right in **Figure 3**. **Figure 6** displays a plot of $\psi_2(x_2, y_2)$ for channel (5) at an energy

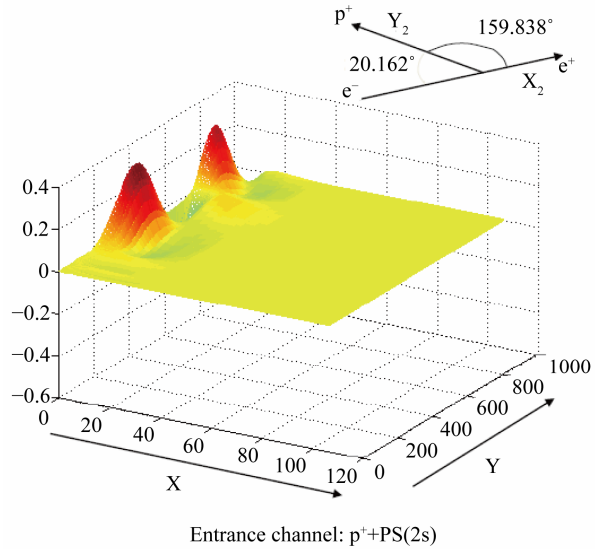

Entrance channel: p⁺+PS(2s)

Figure 4. This is the graph of the wave amplitude in channel 5 at $E_1 = 0.875Ry$ near one of the maximum of σ_{66}. It is noted, the part of the wave amplitude nearest to the target is much longer and wider than that of a De Broglie wave amplitude with the same wavelength displayed in Figure 5.

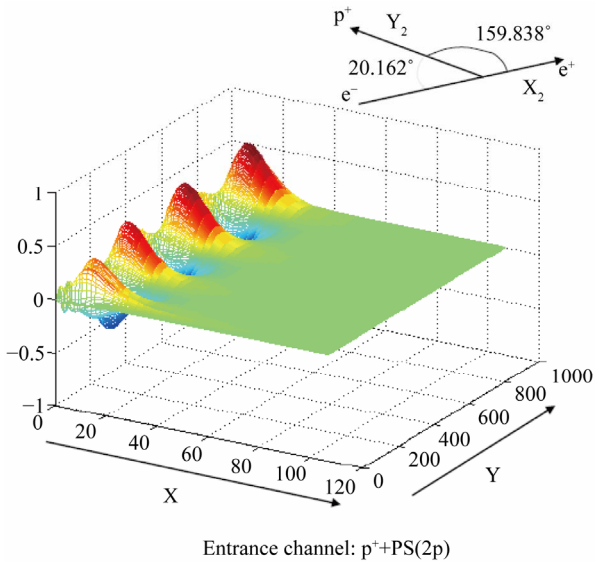

Entrance channel: p⁺+PS(2p)

Figure 5. This is the graph of the wave amplitude in channel 6 at $E_1 = 0.875Ry$. It retains a near normal De Broglie wave structure with $\lambda_1 = 380.85\alpha_0$. However it may change at a slightly different energy.

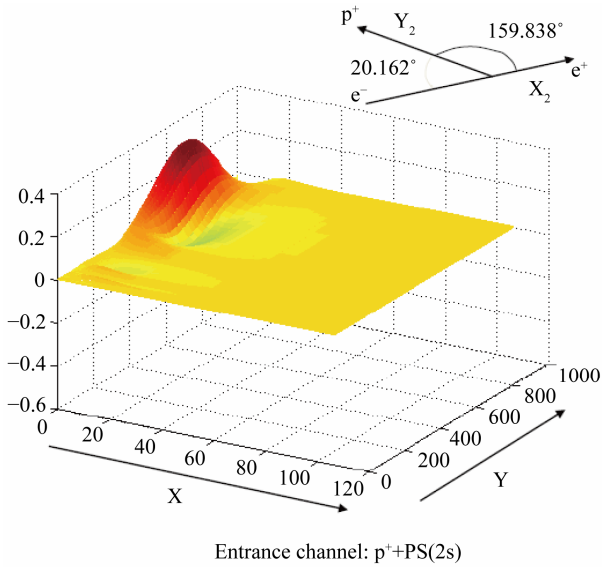

Entrance channel: p⁺+PS(2s)

Figure 6. This is the graph of the wave amplitude in channel 5 at $E_1 = 0.87465Ry$ with $\lambda_2 = 637.34\alpha_0$. It is noted, this wave packet is directly related to the second cross section resonance in Figure 3.

$E_1 = 0.87465Ry$. This energy is near the peak of the second resonance. **Figure 7** displays plot of $\psi_2(x_2, y_2)$ for channel (6) at an energy $E_1 = 0.87454Ry$. This energy is near the peak of the third resonance at the lowest energy end.

A systematic examination of such wave function graphs reveals a simple physical mechanism as the source of the cross section oscillation displayed in **Figure 3**. The Coulomb field of the incoming proton splits the degenerate energy levels of $Ps(n=2, \ell=0)$ and $Ps(n=2, \ell=1)$ into two energy levels, a case of the Stark effect [13], with an energy split $\Delta E = \mu_e \varepsilon_c$. μ_e is the (induced) permanent electric-dipole moment of the Positronium target $Ps(n=2)$, ε_c is the coulomb field of the proton at the target.

Figures 1-6 suggest that resonant excitation of the target energy levels takes place when the channel energy $E = E_5 = E_6$ in atomic energy unit satisfies the following quantum condition:

$$\varepsilon_m = \langle E \rangle_m = m|\mu_e| / \langle y^2 \rangle_m, m = 1,2,3 \qquad (7)$$

ε_m is the channel energy E at the peak of the m^{th} resonance from the cross section graph **Figure 3**.

In the mass-scaled Jacobi coordinate system the electric Dipole moment of $Ps(n=2)$ has the numerical value $|\mu_e| = 23.97389$. y is the radial coordinate of the incoming proton. The meaning of $\langle y^2 \rangle_m$ is defined in the next paragraph.

Figure 1 reveals the underlying physics that enables the resonant transfer of energy from the incoming De Broglie wave to the target. When the colliding system

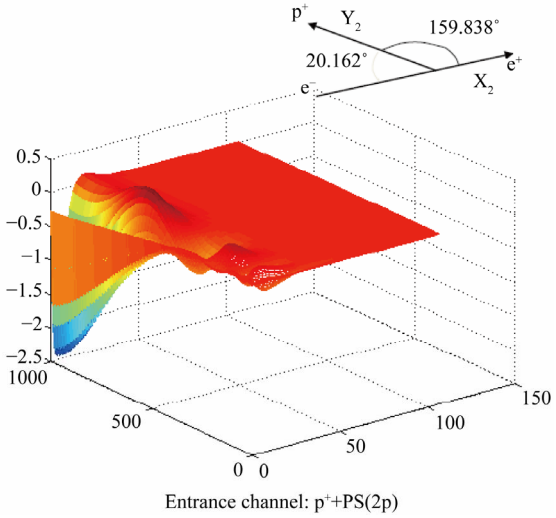

Figure 7. This is the graph of the wave amplitude in channel 6 at $E_1 = 0.87464Ry$ near the third cross section peak with $\lambda_3 = 967.54\alpha_0$. This wave packet is cut-off at $1000\alpha_0$ before it reaches maximum located at ~1305.9 α_0.

approaching the resonant configuration given by Equation (7), **Figure 1** reveals that sudden repulsion compels the incoming De Broglie wave to convert all its energy, ε_m, to a photon which is readily absorbed and sends the target to its excited state while the incoming "particle" is now a De Broglie wave packet centered at a distance $y_m = \sqrt{\langle y^2 \rangle_m}$ from the target. This photon is the quantum equivalent of the well known Bremsstrahlung Radiation generated when a charged particle is subjected to deceleration that distorts the particle's coulombic field lines with transversal components such that an electromagnetic wave is generated.

A dimensionless form of (7) is:

$$y_m/\lambda_m = \sqrt{|\mu_e|m}/2\pi, \text{where } \varepsilon_m = (2\pi/\lambda_m)^2 \qquad (8)$$

λ_m is the De Broglie wave length at energy ε_m.

The wave packets presented in **Figures 4**, **6** and **7**, provide a new way to estimate the life-time, τ_m, of the resonances. Since the De Broglie wave can not return without the disappearance of the wave packets and the return of its energy through a reverse process from that discussed above.

From **Figures 4**, **6** and **7**, the widths of the wave packets are $(\Delta y_m) \approx \lambda_m, m = 1,2,3$ for the first three resonances. An estimate of the life-time τ_m of the resonances can be made using a pair of uncertainty principle. The life-times obtained are as good if not better than that obtained using traditional methods [14], Namely

$$\begin{aligned} &\Delta p_y = 1/\lambda_m, \Delta\varepsilon_m = (\Delta p_y)^2 \text{ in atomic units} \\ &\tau_m = (1/\Delta\varepsilon_m) \times 2.42 \times 10^{-17} \text{ sec} \end{aligned} \qquad (9)$$

From **Figure 3** it is estimated that the peak of the cross section of the three resonances located at the first channel energies $0.875Ry$, $0.87465Ry$ and $0.87454Ry$ for $m = 1,2$ and 3 respectively. The corresponding ε_m of Equation (7) are 2.7218×10^{-4} a.u., 0.9718×10^{-4} a.u. and 0.4217×10^{-4} a.u. for $m = 1,2$ and 3 respectively. Giving ε_m, λ_m, the location of the peak of the wave packet y_m and the life time of the resonance τ_m are calculated and listed in **Table 1**.

Figures 4 and **6** give a three dimensional view of the first two wave packets. It is not easy to project y_m from this orientation. However, using a two dimensional view along the y axis, a good estimate of y_1 and y_2 is made, they agree with the numbers in **Table 1** within a few percent. y_3 is located outside the range of cut-off in **Figure 7**. Direct measurement of y_3 is not possible. Estimated value is consistent with the value in **Table 1**.

4. Estimation of Upper Bounds for Higher Thresholds with $n > 2$

It is unlikely at the present time to calculate all possible resonances. The role these resonances play in the physical world can be better understood from the following consideration. The Stark effect no longer exists when ε_m is larger than the fine structure energy which removes the coulomb degeneracy in the $Ps(n)$ energy levels. **Table 2** lists the fine structure energies for $n = 2,3,4$ where n is the principle quantum number for positronium atom. The corresponding De Broglie wave length λ_f and τ_f are the upper bounds for λ_m and τ_m respectively.

As the collision energy increases the resonances appear near each and every $Ps(n \geq 2)$ thresholds. As n increases, the density of energy levels increases rapidly, **Tables 1** and **2**. Show that λ_m, τ_m increases rather rapidly as well. Equation (8) shows that the center of the wave packet $y_m > \lambda_m$ increases even more rapidly due to the

Table 1. Calculated values of y_m, τ_m from (7)-(9).

m	$\lambda_m(\alpha_0)$	$\Delta\varepsilon_m$(a.u.)	$y_m(\alpha_0)$	τ_m(sec.)
1	380.85	0.00000689	296.8	0.35×10^{-11}
2	637.35	0.00000246	702.4	0.98×10^{-11}
3	967.54	0.00000107	1306.0	2.27×10^{-11}

Table 2. Fine structure energy and upper bounds for λ_m, and τ_m.

n	Fine structure energy (a.u.)	$\lambda_f(\alpha_0)$	τ_f(sec)
2	0.00000104	6161	0.92×10^{-9}
3	0.00000037	10329	2.58×10^{-9}
4	0.00000017	15239	5.62×10^{-9}

increase in electric dipole moments of $Ps(n)$.

Consequently, these resonances enable the three-body colliding system to take up considerable amount of physical space for a time comparable or larger than that of most atomic processes.

5. Discussion

Gailitis and Damburg [2] discussed this type of resonance fifty years ago. For ease of reference, let's call it a Gailitis resonance. The Gailitis resonances appear only slightly above the threshold of a degenerate new channel. This is very different from the much investigated Feshbach resonances which can be found only slightly below such a threshold. As a result, the Gailitis resonances, if found occasionally [1], have been ignored as ghostly structures of numerical calculations. However, advances in supercomputers enable a complete calculation of all the properties of the resonances using the Modified Faddeev Equation without any intermediate approximations. In addition, the wave functions of individual resonances are readily rendered in 3-D graphs. From the graphs, the wave functions reveal much more interesting physics then just the energy and the width of the resonance. A comparison of the properties of these two types of resonances is summarized in **Table 3**.

It is shown that the Gailitis resonances span considerably larger physical space with much longer lifetimes compared to Feshbach resonances. As with Feshbach resonances, Gailitis can also be used as a similar tool to probe nature, but for studying physical spaces and timescales that are comparably larger. The sizes of Gailitis resonances are comparable to nano-particle systems. The lifetimes of Gailitis resonances are comparable to or can exceed that of most atomic processes.

These long lifetimes open up new and interesting possibilities for study. Possible processes involve interactions other than the Coulomb force or possible interactions with the environment external to the three-body system. As an example of the former, consider the three-body coulombic scattering of positron—hydrogen that produces in-flight positron—electron annihilation peaks near every Feshbach resonance as investigated in [15]. The positron-electron annihilation in flight is due to the weak interaction only. The large wave packet formed during the resonant duration is responsible for such external activities. The long lifetime is a direct result of a large wave packet, as described in Sections 3-4.

The Stark-effect is a universal phenomenon. These kind of resonances must occur whenever degeneracy exists in the target in coulombic scattering. Therefore the target is not necessarily an atom. The resonance induced long-range correlations in coulombic scattering systems encourage possible intriguing natural microscopic processes to take place during their life-time.

Table 3. Comparison of properties of Feshbach and Gailitis resonances.

Properties	Feshbach resonance	Gailitis resonance
Underlying physics	Incoming charged particle induces a potential well that is embedded in the Coulomb 3-body system. This potential well produces a series of temporary bound states.	Incoming charged particle induces split of the degenerate energy levels of the target. Resonant excitation between these levels takes place when the target receives a photon via Bremsstrahlung radiation from the incoming particle with an energy that satisfies the quantum Equation (7)
Energy of resonances	Just below the thresholds of a new channel by an amount less than the fine structure energy	Just above the thresholds of a new channel by an amount less than the fine structure energy
Distance between the target and the incoming "charged particle" wave packet at resonance	On the order of hundreds of Bohr radii or less	Can be thousands of Bohr radii (See **Table 1** for y_m and **Table 2** and Equation (8) for estimated higher threshold resonances)
Lifetime	~10^{-13} sec or less [7]	~10^{-11} sec or longer (see **Table 1** for calculated results and see **Table 2** for estimated values at higher threshold resonances)

6. Acknowledgements

The authors thank Dr. Anand Bhatia for helpful discussions. This work is supported by a generous XSEDE resource allocation from the Texas Advanced Computer Center (TACC), at the University of Texas, Austin.

REFERENCES

[1] C. Y. Hu, D. Caballero and Z. Papp, *Physical Review Letters*, Vol. 88, 2002, Article ID: 063401. doi:10.1103/PhysRevLett.88.063401

[2] M. Gailitis and R. Damburg, *Journal of Experimental and Theoretical Physics*, Vol. 17, 1963, p. 1107.

[3] N. Levinson, K. Dan and S. Vidensk, *Matematisk-Fysiske Meddelelser Konglige Danske*, Vol. 25, 1949, p. 9.

[4] A. K. Bhatia, *Physical Review A*, Vol. 9, 1974, p. 9. doi:10.1103/PhysRevA.9.9

[5] A. K. Bhatia and Temkin, *Physical Review A*, Vol. 11, 1975, p. 2018. doi:10.1103/PhysRevA.11.2018

[6] Y. K. Ho, Bhatia and Temkin, *Physical Review A*, Vol. 15, 1977, p. 1423. doi:10.1103/PhysRevA.15.1423

[7] Y. K. Ho, *Physical Review A*, Vol. 35, 1987, p. 3169. doi:10.1103/PhysRevA.35.3169

[8] T. T. Gien, *Journal of Physics B*, Vol. 29, 1996, p. 2127. doi:10.1088/0953-4075/29/10/020

[9] Z. C. Yan and Y. K. Ho, *Physical Review A*, Vol. 77, 2008, Article ID: 030701.

[10] A. K. Bhatia, *Physical Review A*, Vol. 86A, 2012, Article ID: 032709.

[11] C. Y. Hu, *Journal of Physics B*: *Atomic, Molecular and Optical Physics*, Vol. 32, 1999, p. 3077. doi:10.1088/0953-4075/32/12/323

[12] C.-Y. Hu, *Physical Review A*, Vol. 59, 1999, p. 4813. doi:10.1103/PhysRevA.59.4813

[13] L. I. Shiff, *Quantum Mechanics*, Vol. 156-158, 1949.

[14] C. Y. Hu, S. L. Yakovlev and Z. Papp, *Nuclear Instruments and Methods in Physics Research*, Vol. B247, 2006, p. 25.

[15] S. L. Yakovlev, C. Y. Hu and D. Caballero, *Journal of Physics B*: *Atomic*, *Molecular and Optical Physics*, Vol. 40, 2007, p. 1675. doi:10.1088/0953-4075/40/10/003

